Slight structural modulation around a pivotal bond: high impact on enantiomeric stability

Daniel Farran, Nicolas Vanthuyne, Giulia Bossa, Vincent Belot, Muriel Albalat, Marion Jean, Christian Roussel

▶ **To cite this version:**

Daniel Farran, Nicolas Vanthuyne, Giulia Bossa, Vincent Belot, Muriel Albalat, et al.. Slight structural modulation around a pivotal bond: high impact on enantiomeric stability. New Journal of Chemistry, 2021, 45 (35), pp.16039-16047. ⟨10.1039/d1nj03178c⟩. ⟨hal-03516890⟩

HAL Id: hal-03516890

https://hal.science/hal-03516890v1

Submitted on 7 Jan 2022

HAL is a multi-disciplinary open access archive for the deposit and dissemination of scientific research documents, whether they are published or not. The documents may come from teaching and research institutions in France or abroad, or from public or private research centers.

L'archive ouverte pluridisciplinaire **HAL**, est destinée au dépôt et à la diffusion de documents scientifiques de niveau recherche, publiés ou non, émanant des établissements d'enseignement et de recherche français ou étrangers, des laboratoires publics ou privés.

HAL Authorization

Slight structural modulation around a pivotal bond: High impact on enantiomeric stability

Daniel Farran,* Nicolas Vanthuyne, Giulia Bossa, Vincent Belot, Muriel Albalat, Marion Jean, Christian Roussel

Aix Marseille Univ, CNRS, Centrale Marseille, iSm2, Marseille, France

* *Corresponding author's e-mail address : daniel.farran@univ-amu.fr*

ABSTRACT:

Based on a *N*-arylthiazoline scaffold, 22 structures with a N-C_{aryl} chiral axis were synthesized exhibiting a huge molecular diversity for the four flanking substituents around the pivotal bond. The determination of their corresponding rotational barriers by thermal kinetic experiments or from the analysis of plateau shape chiral HPLC chromatogram allowed to rank these compounds according to their enantiomeric stability : 4 rotamers, 5 isolable atropisomers (i.e. not enough robust to be handled without risk of racemization) and 13 stable atropisomers. The influence of the flanking substituents was investigated showing that a minor structural modification may result in a drastic change on the value of the rotational barrier. All these results offer a set data on structure-rotational barrier relationships very helpful to design molecules exhibiting chiral axis or to optimize the enantiomeric stability of such structure. To complete this study, the racemization pathways were examined thanks to X-Ray analysis and DFT calculations, highlighting the importance of the aromatic ring distortion during the transition state on the energetic cost of the rotation.

INTRODUCTION

According IUPAC, atropisomers are defined as "a subclass of conformers that can be isolated as separate chemical species and which arise from restricted rotation about a single bond".[1] For instance, atropisomers are observed in the presence of a chiral axis i.e. "an axis about which a set of ligands is held so that it results in a spatial arrangement that is not superposable on its mirror image" and lead consequently to a pair of enantiomers. During the last decades, chemists took advantages of this type of chirality to develop molecules exhibiting very high potential,[2] especially in homogenous asymmetric catalysis.[3] However, since this stereoisomerism depends on a dynamic process of interconversion between both enantiomers, such structures were not considered as appropriate for a pharmaceutical purpose. Very recently, this dogma was challenged by medicinal chemists due to the need to explore a larger chemical space for drug candidates.[4,5] Thus, the concept of atropisomerism was revealed as an exciting issue in drug discovery with promising opportunities.

The dynamic aspect of atropisomerism has to be addressed with high care during the design and the optimization of molecules such as drugs or catalysts. The Oki's precept[6] is often recalled to fix the border between rotamers (fast rotation) and atropisomers (restricted

---

[1] IUPAC*, Compendium of Chemical Terminology, version 2.3.3*, **2014**, pp 126 and 270.

[2] a) M. Mancinelli, G. Bencivenni, D. Pecorari, A. Mazzanti, *Eur. J. Org. Chem.* **2020**, 4070–4086; b) E. Kumarasamy, R. Raghunathan, M. P. Sibi, J. Sivaguru *Chem. Rev.* **2015**, *115*, 11239−11300.

[3] a) M. Berthod, G. Mignani, G. Woodward, M. Lemaire, *Chem. Rev.* **2005**, *105*, 1801-1836; b) Y. Chen, S. Yekta, A. K. Yudin, *Chem. Rev.* **2003**, *103*, 3155-3211.

[4] a) M. M. Cardenas, A. D. Nguyen, Z. E. Brown, B. S. Heydari, B. S. Heydari, S. D. Vaidya, J. L. Gustafson, *Arkivoc* **2021**, 20-47; b) S. T. Toenjes, J. L. Gustafson, *Future Med. Chem.* **2018**, *10*, 409-422; c) P. W. Glunz, *Bioorg. Med. Chem. Lett.* **2018**, *28*, 53-60; d) J. Chandrasekhar, R. Dick, J. Van Veldhuizen, D. Koditek, E.-I. Lepist, M. E. McGrath, L. Patel, G. Phillips, K. Sedillo, J. R. Somoza, J. Therrien, N. A. Till, J. Treiberg, A. G. Villasenor, Y. Zherebina, S. Perrault, *J. Med. Chem.* **2018**, *61*, 6858-6868; e) D. E. Smith, I. Marquez, M. E. Lokensgard, A. L. Rheingold, D. A. Hecht, J. L. Gustafson, *Angew. Chem. Int. Ed.* **2015**, *54*, 11754-11759; f) J. E. Smyth, N. M. Butler, P. A. Keller, *Nat. Prod. Rep.* **2015**, *32*, 1562-1583.

[5] a) S. R. LaPlante, P. J. Edwards, L. D. Fader, A. Jakalian, O. Hucke, *ChemMedChem* **2011**, *6*, 505-513; b) S. R. LaPlante, L. D. Fader, K. R. Fandrick, D. R. Fandrick, O. Hucke, R. Kemper, S. P. F. Miller, P. J. Edwards, *J. Med. Chem.* **2011**, *54*, 7005-7022; c) J. Clayden, W. J. Moran, P. J. Edwards, S. R. LaPlante, *Angew. Chem., Int. Ed.* **2009**, *48*, 6398–6401.

[6] M. Oki, *Top. Stereochem.* **1983**, *14*, 1-81.

rotation): it states that atropisomerism concerns isolable isomers with a half-life time of interconversion of at least 1000 seconds corresponding to a rotational barrier of 92.8 kJ/mol at 25°C. This statement is convenient but not entirely satisfactory mainly because not enough accurate regarding the feature "isolable" of a pure enantiomer. Laplante et al. proposed a practical approach to tackle this issue: stereoisomers possessing a chiral axis are classified into three groups depending on their rotational barriers.[5] Class I consists of rotamers that spin fast about chiral axis from one conformer to the other. Class III includes enantiomeric stable atropisomers which have to be seen similarly to unracemizable enantiomers. Finally, atropisomers with intermediate enantiomeric stability are comprised in class II; these compounds can be isolated but under specific conditions (such as low temperature) which makes impossible their use for a given application. Herein, we classified compounds with chiral axis according a similar ranking, taking in mind that the boundary between two consecutive groups should be envisaged as slightly flexible in order to adjust to the intended purpose of the molecule. For instance, a catalyst with a chiral axis operating in a reaction at room temperature can be considered as a stable atropisomer when its rotational barrier is greater than 115 kJ/mol (i.e. a half-life time of 91 days at 25°C).

The aim of this paper is to highlight that a minor structural modification introduced close to a chiral axis generates major outcomes on the enantiomeric stability of an atropisomer. Although many rotational barriers are reported in literature,[7] few studies have been carried out on series of compounds in order to evaluate the impact of molecular diversity on $\Delta G^{\neq}_{rot}$ values.[8,9] The set of results reported hereafter provides some general trends on the

[7] I. Alkorta, J. Elguero, C. Roussel, N. Vanthuyne, P. Piras, *Adv. Heterocycl. Chem.* **2012**, *105*, 1-188.
[8] V. Belot, D. Farran, M. Jean, M. Albalat, N. Vanthuyne, C. Roussel, *J. Org. Chem.* **2017**, *82*, 10188-10200.
[9] a) G. Bott, L. D. Field, S. Sternhell, *J. Am. Chem. Soc.* **1980**, *102*, 5618-5626; b) R. Ruzziconi, S. Spizzichino, L. Lunazzi, A. Mazzanti, M. Schlosser, *Chem. Eur. J.* **2009**, *15*, 2645-2652; c) Ö. D. Ordu, I. Dogan, *Tetrahedron: Asymmetry* **2004**, *15*, 925-933.

structure-rotational barrier relationship. These data are of significant importance in the design and the structure optimization for compounds of interest: structural modifications can be envisaged to modulate the rotational barrier either by increasing it to access stable atropisomers or by decreasing it to lead to rotamers developed as single flexible compounds. To achieve our goal, a *N*-arylthiazoline template (Figure 1) with a restricted rotation about the N-C_{aryl} bond appears extremely appropriate. In these series, the resulting rotational barriers represent a proper view of the steric bulk of substituents borne on the blocking positions around the pivotal bond, whereas the contribution of electronic aspects is negligible.[8] In addition, the barriers to rotation on this scaffold are very sensitive to steric variations giving rise to a large range of $\Delta G^{\neq}_{rot}$ and providing compounds belonging to each of the three classes of stereoisomers mentioned previously.[10] Moreover, the rotational barrier is weakly dependent of the temperature as demonstrated by the small and constant entropy parameters.[8] Thus, this homogenous series can be considered as reliable to compare rotational barriers even if they are not evaluated exactly at the same temperature. Besides these crucial points, it is worth noting that a huge molecular diversity is easily accessible on *N*-arylthiazolines since they are synthesized from commercially available ortho-substituted anilines and α-halogeno ketones.

[10] N. Vanthuyne, F. Andreoli, S. Fernandez, M. Roman, C. Roussel, *Lett. Org. Chem.* **2005**, *2*, 433-443.

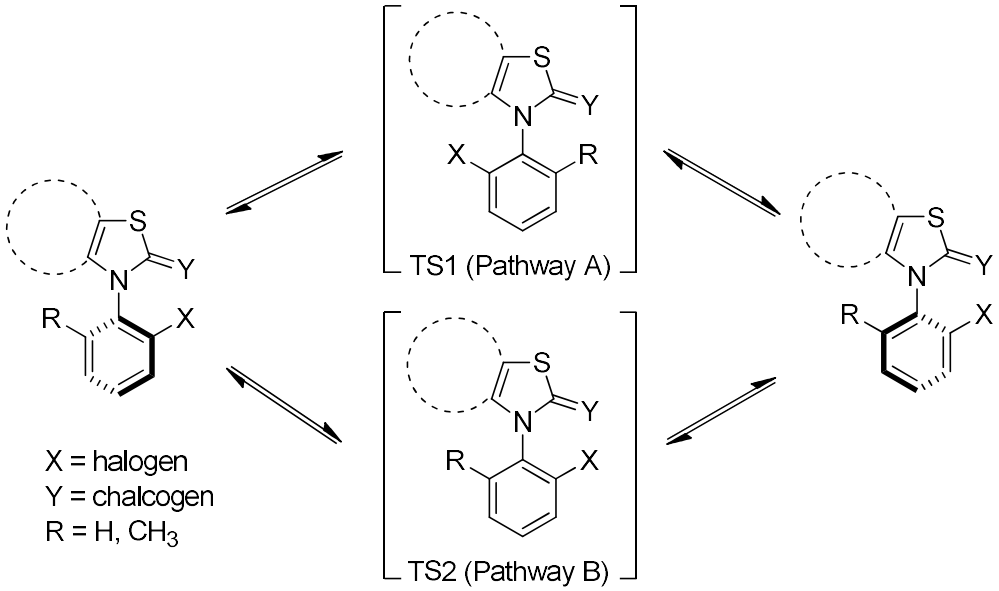

Figure 1. Racemization in *N*-arylthiazoline series

RESULTS AND DISCUSSION

The ortho halogenated *N*-arylthiazoline-2-thiones **1** represent a relevant starting point since a wide range of values of rotational barriers is covered from the fluoro derivative **1a** to the iodo compound **1d** (Table 1). A plateau shape was observed during liquid chromatography on a chiral stationary phase for compound **1a** and the corresponding barrier to rotation was estimated at 82.5 kJ/mol according to the Trapp and Schurig equation,[11] implying that **1a** belongs to the class II. The three other structures are included in class III due to the higher steric demand of their respective halogen atoms compared to the fluorine.

[11] O. Trapp, V. Schurig, *Chirality* **2002**, *14*, 465-470.

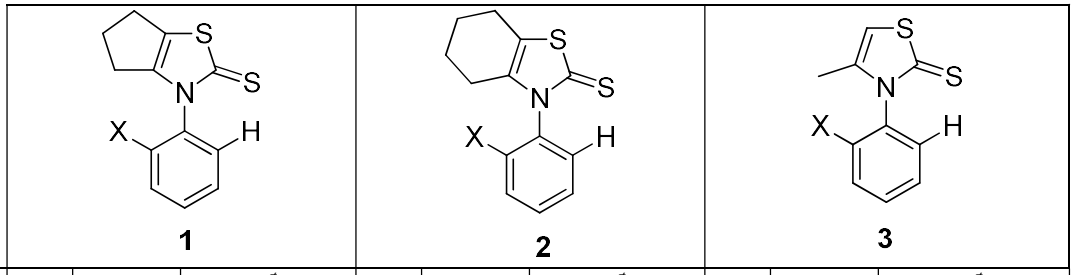

X	1	$\Delta G^{\neq}_{rot}$	$\Delta G^{\neq}_{calc}$ via A[c]	$\Delta G^{\neq}_{calc}$ via B[c]	2	$\Delta G^{\neq}_{rot}$	$\Delta G^{\neq}_{calc}$ via A[c]	$\Delta G^{\neq}_{calc}$ via B[c]	3	$\Delta G^{\neq}_{rot}$	$\Delta G^{\neq}_{calc}$ via A[c]	$\Delta G^{\neq}_{calc}$ via B[c]
F	**1a**	**82.5**	83.7	112.9	**2a**	**113.7**	113.7	143.1	**3a**	**114.7**	117.2	138.2
Cl	**1b**	**133.3**	137.8	154.1	**2b**	**159.2**	163.7	175.2	**3b**	**161.6**	167.5	173.8
Br	**1c**	**145.5**	152.3	163.1	**2c**	**165.9**	175.2	181.0	**3c**	**167.3**	178.4	179.9
I	**1d**	**155.5**	167.4	171.6	**2d**	**168.1**	189.5	189.4	**3d**	**168.6**	191.6	187.4

[a]Rotational barriers are reported in kJ/mol.
[b]Solvent and temperature are given in supporting information.
[c]Calculated rotational barriers through pathway A or B using PBE0 functional and def2-TZVPP basis set.

Table 1. Rotational barriers of ortho halogenated *N*-arylthiazoline-2-thiones[a,b]

Density functional theory (DFT) calculations were performed for series **1** using three different functional/basis sets: B3LYP/6-311G(3d,3p), M06-2X/6-311G(3d,3p) and PBE0/def2-TZVPP.[12] Calculations provided the barriers and allowed to explore the energies associated to the two possible pathways for the rotation about the pivotal N-C_{aryl} bond (Figure 2). During the rotation, the *N*-aryl ortho halogen is passing in front of the methylene group (Figure 2: pathway A) or in front of the sulphur atom (Figure 2: pathway B). Whatever the method employed, calculated barriers are in line with experimental ones, PBE0/def2-TZVPP reproducing the experimental data most closely (Table 1). Previous experimental data from the steric scale based on a *N*-arylthiazoline-2-thione scaffold gave a methyl group bigger than a chlorine which allowed to hypothesize none Cl/S electrostatic repulsion in the TS and thus suggested that the racemization proceeds through the transition state 1 (TS1) in

[12] DFT calculated energies and the computational details are given in the supporting information

series **1**.[8] This assumption was supported by the calculations achieved herein which gave the pathway A as the most favourable with a lower energetic cost.

From these preliminary results, an expanded study to the whole four flanking substituents was carried out, and we first concentrated our efforts on the cyclopentene borne by the thiazoline core. Two modifications were envisioned on this moiety of the skeleton: the extension to a six-membered carbocycle (series **2**) and the removal of the carbocycle accompanied by the installation of a methyl in position 4 of the thiazoline ring (series **3**).[13] The syntheses of the desired *N*-(o-substituted-phenyl)-thiazoline-2-thiones were achieved using a protocol previously described:[8] treatment of ortho-halogenated aniline with carbon disulfide to generate the dithiocarbamate salt which was allowed to react with 2-chlorocyclohexanone or chloroacetone to furnish **2** or **3** respectively. Preparative HPLC on chiral support on the so-called (*S*,*S*) Whelk-O1 column provided both enantiomers and rotational barriers were then determined by kinetic study of the thermal racemisation of atropisomers at a given temperature. The kinetic studies were carried out in similar solvents (chlorobenzene, 1,2-dichlorobenzene or 1,2,4-trichlorobenzene) to eliminate misinterpretation caused by a hypothetical solvent effect. The resulting Gibbs free energies of activation $\Delta G^{\neq}_{rot}$ were obtained from the Eyring equation and are gathered in Table 1.

For a given halogen atom in ortho position, compounds **2** and **3** possess very similar rotational barriers. We obtained a $\Delta G^{\neq}_{rot}$ value for compound **2b** of 159.2 kJ/mol in 1,2-dichlorobenzene at 180°C vs 161.6 kJ/mol for **3b** under the same conditions. These very close results revealed that substituents in position 4 on the thiazoline ring of **2** and **3**, i.e. methylene of a six-membered ring and methyl respectively, exhibited a similar spatial requirement. Moreover, these two structural modifications increased notably the rotational

[13] For a study about the influence of the ring size on the rotational barrier of an atropisomers series see: J. E. Diaz, A. Mazzanti, L. R. Orelli, M. Mancinelli, *ACS Omega* **2019**, *4*, 4712-4720.

barriers compared to homologues **1**. A significant example concerns compounds **1a** and **2a** that only differ by one atom on the size of their carbocycles. This minor modulation generated a noteworthy increase of 31.2 kJ/mol between the $\Delta G^{\neq}_{rot}$ of **1a** and **2a**, and allowed moving from the class I/class II border to the class II/class III one.

Careful examinations of the structures obtained by X-Ray crystal analyses of the three *N*-(o-bromophenyl)-thiazoline-2-thiones **1c**, **2c** and **3c** help to rationalize experimental $\Delta G^{\neq}_{rot}$ values (Figure 2). The resulting rotational barriers are directly connected to the angle between the endocyclic nitrogen atom and the substituent borne in position 4 of the thiazoline ring. This angle was measured at 120.4° for 4-methyl thiazoline-2-thione **3c** and 122.3° for the six-membered ring derivative **2c**, compared to 131.8° found for the five-membered ring homologue **1c** leading to a much easier rotation around the pivotal bond in this latter case.

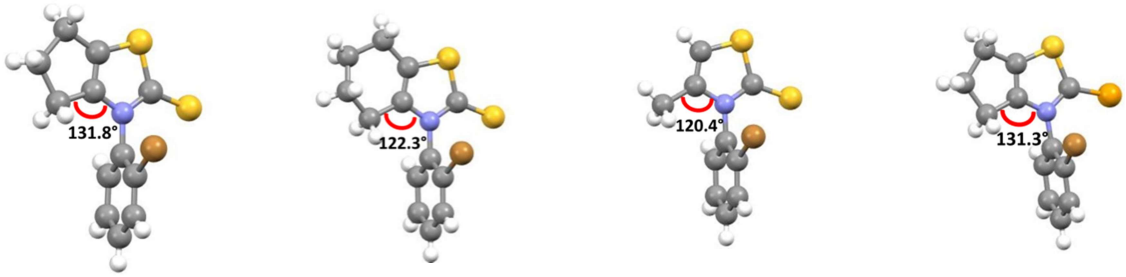

(S_a)-**1c** (S_a)-**2c** (S_a)-**3c** (S_a)-**6c**

Figure 2. X-Ray structures of the (S_a) enantiomer of bromo derivatives

DFT-calculated data reproduced properly the experimental $\Delta G^{\neq}_{rot}$ for these two new series **2** and **3** (Table 1), although $\Delta G^{\neq}_{calc}$ for iodo derivatives **2d** and **3d** are overestimated whatever the level of theory used.[12] Nevertheless, despite this deviation, it is important to mention

that the general evolution of $\Delta G^{\neq}_{calc}$ values in both series, from the fluoro derivative to the iodo derivative, matches suitably to experimental results given the wide range of the corresponding rotational barriers.[14] As noticed for series **1**, calculations indicated that the racemization mechanism proceed via TS1, except for compounds **2d** and **3c** for which any assumptions may not be stated due to insignificant energy gap between pathways A vs B, and also for **3d**, for which the computational study suggests the opposite racemization mechanism via TS2.[15] It is particularly interesting to focus on this latter aspect since it helps to elucidate an experimental result which can be considered as odd at the first sight: $\Delta G^{\neq}_{rot}$ of **3d** (168.6 kJ/mol in 1,2,4-trichlorobenzene at 214°C) similar to $\Delta G^{\neq}_{rot}$ of **3c** (167.3 kJ/mol in 1,2,4-trichlorobenzene at 214°C), i.e. a difference of only 1.3 kJ/mol despite the higher steric demand of an iodine vs a bromine. A plot of enantiomerization barriers of series **1** vs series **3** allows to detect a peculiar behaviour for compound **3d** which accounts for the poor correlation (Figure 4; r^2= 0.9702 for the whole data vs r^2 = 0.9928 without iodine derivatives; red solid line represents linear regression for F, Cl and Br derivatives). In this context, the comparison of the rotational barrier of **3d** to the three others compounds of series **3** requires special care since two different racemization pathways are presumably involved. The same trend seems to emerge when comparing series **1** to series **2** (Figure 4; r^2= 0.9797 for the whole data vs r^2 = 0.9957 without iodine derivatives; blue solid line represents linear regression for F, Cl and Br derivatives), but the phenomenon is here less significant and does not allowed to clearly rule for a reverse racemization pathway for **2d** versus **2a-c**.

A peripheral unexpected aspect raised by the plotting depicted on Figure 3 concerns the amplitude on the $\Delta G^{\neq}_{rot}$ value involved by identical structural modifications carried out on

[14] Plots of experimental versus calculated values are available in the supporting information.

[15] Same trend observed with three different functional/basis sets (B3LYP/6-311G(3d,3p), M06-2X/6-311G(3d,3p) and PBE0/def2-TZVPP): see supporting information.

different series. Indeed, the rotational barriers for series **1** exhibited a greater sensitivity to the size of the ortho substituent than the six-membered ring and 4-Me derivatives, **2** and **3** series respectively, as showed by the slope of the linear regression which is > 1 when comparing the five-membered ring fluoro, chloro and bromo derivatives with their homologues.

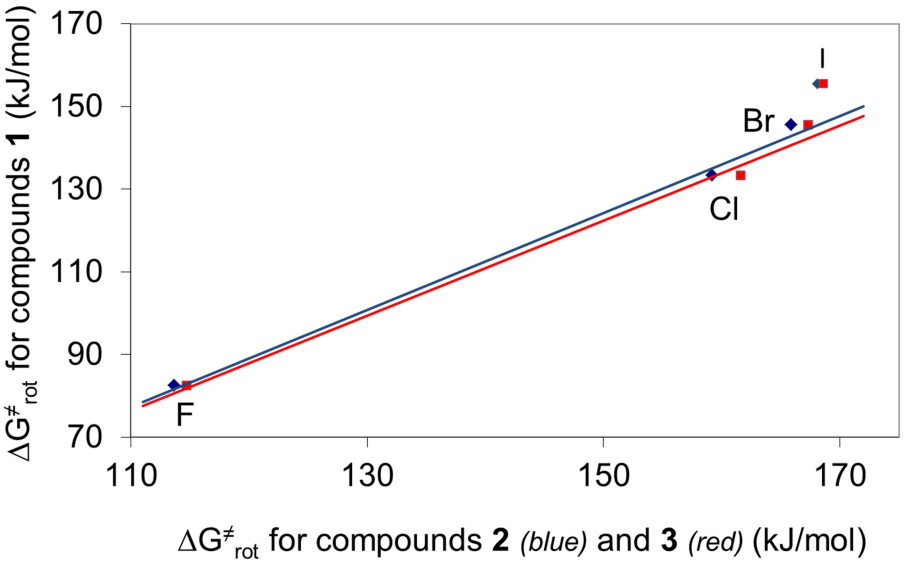

Figure 3. Experimental rotational barriers for series **1** vs series **2** and **3**

To gain understanding on the conformational parameters involved in the two possible rotational pathways, information on molecular geometries can be gleaned from the computational study. The values for angles between the bonds bearing a flanking substituent and the bond connected to the chiral axis (Figure 4: angles α, β and γ), as well as the torsion of the aromatic ring (dihedral angle ψ : C1'-C6'-C4'-C3' in Figure 4), the dihedral angle between the thiazoline ring and the aromatic ring (dihedral angle ϕ : C2-N3-C1'-C6' in Figure 4) and the pivotal bond length C1'-N3 are gathered in the supporting information, both for ground and transition states. These crucial parameters for the mechanism of the

rotation revealed that series **1**, **2** and **3** exhibit the same behaviour which is described hereafter.

The optimized structures for the ground state (GS) showed that the aryl ring was twisted with respect to the heterocyclic ring with C2-N3-C1'-C6' dihedral angles ϕ from 67° to 86°. The geometry of the thiazoline moiety is identical within a series, displaying none impact of the halogen atom. On the aromatic ring, a same variation for angle γ is noticed in all series (from 119° for fluoro derivatives to 121° for iodo derivatives) which can be assigned to the increased steric bulk of the halogen atom. It is also noteworthy that all these angles as well as C1'-N3 bond lengths are in perfect agreement to those revealed by crystal structures.

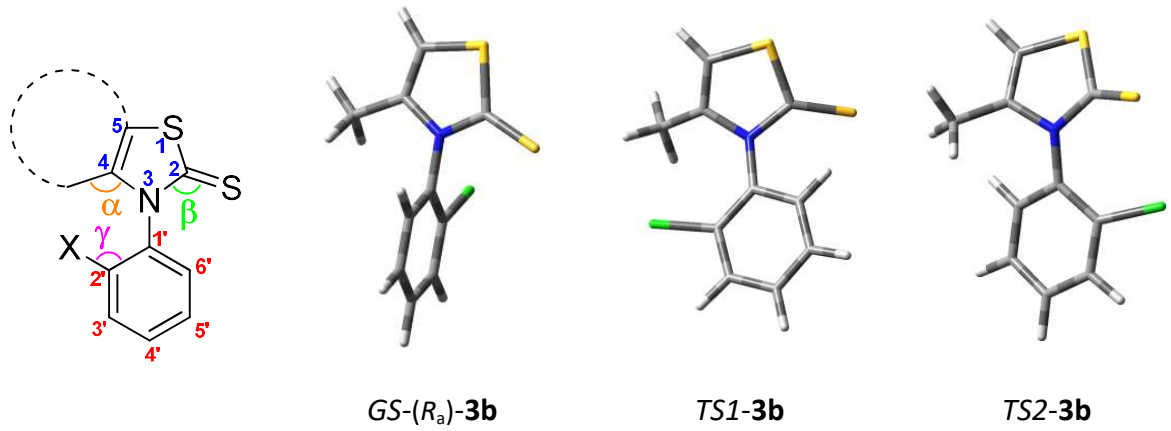

GS-(R_a)-**3b** *TS1*-**3b** *TS2*-**3b**

Figure 4. Atom numbering in *N*-arylthiazoline and GS/TS for **3b**

As expected, the transition states are almost planar. Compared to GS, none significant stretch is observed for the pivotal bond N3-C1'; on the other hand, angles α, β and γ are wider, accompanied by torsions of thiazoline and aromatic rings to allow the rotation around the chiral axis avoiding clashes (Figure 4).

Within a series, the angles α and β are constant for a given racemization pathway, without any influence of the halogen atom borne by the aromatic ring: the values of α and β are characteristic of the thiazoline pattern. Moreover, the angles γ are analogous for all the structures bearing the same halogen regardless the series and the racemization pathway: the values of γ are characteristic of the aromatic pattern. Thus both moieties of the *N*-arylthiazoline-2-thiones behave independently of each other: the TS geometries of the thiazolinethione ring are governed by the five membered ring/six membered ring/methyl substituents, while the nature of the halogen atom controls the TS geometries of the aromatic ring.

For a given *N*-arylthiazoline-2-thione, the values of angle γ are similar in both transition states (e.g. for **3b**: 127.4° in TS1 vs 127.2° in TS2), whereas pathway A lead to higher values for angles α and β than pathway B (e.g. angle α/angle β for **2b**: 125.6°/132.6° in TS1 vs 123.1°/129.9° in TS2). In contrast, the torsion of the aromatic ring is greater for TS2 than TS1 (e.g. C1'-C6'-C4'-C3' dihedral angle ψ for **2b**: 4.8° in TS1 vs 7.4° in TS2) resulting in a higher energy penalty in the former case. Taking into account that the computational study argues in favour of a racemization mechanism via pathway A for compounds **1a-d**, **2a-c** and **3a-b**, the energetic cost for the twist of the aromatic ring appears significant for the racemization process. Interestingly, the torsion of the aromatic ring is similar in TS1/TS2 for **2d** (C1'-C6'-C4'-C3' dihedral angle ψ: 8.1° in TS1 vs 8.5° in TS2), which could explain that none hypothesis on the racemization pathway may be established from calculations in this case.

In order to go further in the structure-rotational barrier relationship, we then investigated two related compounds to previous series. Compound **4d** displays two hydrogen atoms in position 4 and 5 of the thiazoline ring (Table 2). Despite the presence of an iodine atom in ortho-aryl position, the corresponding HPLC profile provided a single peak on several chiral

stationary phases at 10°C,[16] meaning a rotational barrier lower than 80 kJ/mol. Compound **4d** unambiguously belongs to class I, while the three iodo derivatives **1d**, **2d** and **3d** are clearly ranked in class III. This demonstrates the minimal requirement of three substituents (different from hydrogen atoms) on the four flanking positions to access to a configurationally stable thiazoline-2-thione scaffold. Calculation using the appropriate PBE0/def2-TZVPP method furnished a $\Delta G^{\neq}_{calc}$ of 77.3 kJ/mol for **4d**, with a quasi-planar transition state involving I/H5 and Harom/S interactions as expected (pathway A).

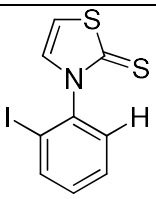

4d

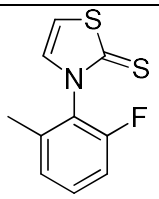

5a

$\Delta G^{\neq}_{rot}$	$\Delta G^{\neq}_{calc}$ via A[c]	$\Delta G^{\neq}_{calc}$ via B[c]	$\Delta G^{\neq}_{rot}$	$\Delta G^{\neq}_{calc}$ via A[c]	$\Delta G^{\neq}_{calc}$ via B[c]
< 80	77.3	149.8	**142.1**	152.9	153,1

[a]Rotational barriers are reported in kJ/mol.
[b]Solvent and temperature are given in supporting information.
[c]Calculated rotational barriers through pathway A or B using PBE0 functional and def2-TZVPP basis set.

Table 2. Rotational barriers of ortho halogenated *N*-arylthiazoline-2-thiones **4d** and **5a**[a,b]

Comparison of rotational barriers between compounds **3a** (114.7 kJ/mol in 1,2-dichlorobenzene at 62°C) and **5a** (142.1 kJ/mol in 1,2-dichlorobenzene at 180°C) offers another set of attractive results. In these two structures, the four substituents around the pivotal bond are identical, but they are not arranged in the same way: the methyl is linked to the C4 of the thiazoline ring in **3a** whereas it is borne in ortho-aryl position for **5a**. In both cases, the corresponding compounds belong to class III. However, this minor modulation on

[16] Attempts of enantiomers separation performed on the following immobilized CSPs: Chiralpak IA, Chiralpak IB, Chiralpak IC, Chiralpak ID, Chiralpak IE and Chiralpak IF.

the skeletons induced an impressive gap of 27.4 kJ/mol on the $\Delta G^{\neq}_{rot}$ value. An additional consequence to this slight structural change was revealed during chiral HPLC analysis: the two enantiomers of **3a** were well resolved on the (*S*,*S*) Whelk-O1 column (α = 1.49 and Rs = 6.65, 25 °C, Heptane/isopropanol/dichloromethane 70/20/10, 1 mL/min) whereas none enantio discrimination was noticed for **5a** in the same conditions, illustrating a perturbation of the interaction between the chiral stationary phase and the analyte in this last case.[17]

The DFT-calculated $\Delta G^{\neq}_{calc}$ for **3a** and **5a** are in accordance with the experimental results. However, although the computational study supports unambiguously pathway A for the racemization process of **3a**, calculated rotational barriers via TS1 and TS2 are too close to plead for one of the two pathways in the case of compound **5a**. Moreover, the geometries of both transition states of **5a** highlighted an important torsion of the aromatic ring (C1'-C6'-C4'-C3' dihedral angle ψ for **5a**: 11.7° in TS1 and 10.3° in TS2, to be compared to 1.9° in TS1 for **3a**) which explains the extra energy required for the rotation of **5a** (Figure 5).

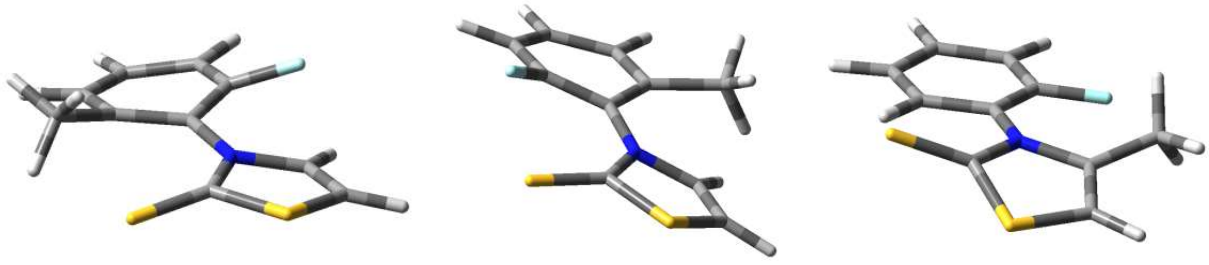

TS1-**5a** *TS2*-**5a** *TS1*-**3a**

Figure 5. Significant distortion on the aromatic moiety in both TS for **5a** vs quasi-planar aromatic ring in the most favourable TS for **3a**

[17] W. H. Pirkle, M. E. Koscho, Z. Wu, *J. Chromatogr. A* **1996**, *726*, 91-97.

Studies were finally directed towards the nature of the exocyclic chalcogen (Table 3). In order to investigate the impact of such modification, ortho halogenated *N*-arylthiazolineselenones **6** and *N*-arylthiazolinones **7** were synthesized.[18] The parent thiazolinethiones **1** were converted into their corresponding thiazolium salts by addition of methyl iodide. This intermediate salt allowed to access to the two targeted series: treatment with sodium hydrogen selenide (obtained by reduction of selenium with sodium borohydride) furnished the desired selenones **6**[19] whereas a subsequent reaction with sodium methylate provided the oxygenated derivatives **7**.[20]

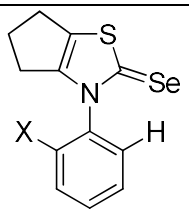

6

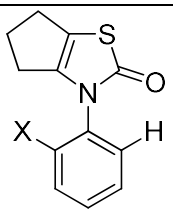

7

X	**6**	$\Delta G^{\neq}_{rot}$	$\Delta G^{\neq}_{calc}$ via A[c]	$\Delta G^{\neq}_{calc}$ via B[c]	**7**	$\Delta G^{\neq}_{rot}$	$\Delta G^{\neq}_{calc}$ via A[c]	$\Delta G^{\neq}_{calc}$ via B[c]
F	**6a**	**85.1**	86.1	118.4	**7a**	**< 80**	56.1	78.2
Cl	**6b**	**134.8**	140.5	163.5	**7b**	**103.2**	102.6	109.3
Br	**6c**	**146.4**	154.9	173.4	**7c**	**109.7**	116.6	116.3
I	**6d**	**155.2**	170.5	184.2	**7d**	**112.0**	133.6	123.0

[a]Rotational barriers are reported in kJ/mol.
[b]Solvent and temperature are given in supporting information.
[c]Calculated rotational barriers through pathway A or B using PBE0 functional and def2-TZVPP basis set.

Table 3. Rotational barriers of ortho halogenated *N*-arylthiazoline-2-selenones **6** and *N*-arylthiazoline-2-ones **7**[a,b]

[18] See supporting information.
[19] a) N. Bellec, D. Lorcy, A. Robert, *Synthesis* **1998**, 1442-1446; b) N. Bellec, D. Lorcy, A. Robert, R. Carlier, A. Tallec, C. Rimbaud, L. Ouahab, R. Clerac, P. Delhaes, *Adv. Mater.* **1997**, *9*, 1052-1056.
[20] a) N. Vanthuyne, F. Andreoli, S. Fernandez, M. Roman, C. Roussel, *Lett. Org. Chem.* **2005**, *2*, 433-443. b) C. Roussel, M. Adjimi, A. Chemlal, A. Djafri, *J. Org. Chem.* **1988**, *53*, 5076-5080.

The corresponding barriers to rotation were measured as described above and revealed very close values when comparing results from sulphur series **1** to selenium series **6**. For example, compounds bearing a bromine atom in ortho-aryl position exhibited $\Delta G^{\neq}_{rot}$ of 145.5 kJ/mol and 146.4 kJ/mol (both in 1,2-dichlorobenzene at 180°C) for **1c** and **6c** respectively, i.e. a difference of merely 0.9 kJ/mol. This similar behaviour is consistent with a comparable steric bulk between sulphur and selenium (van der Waals radii: S = 180 pm and Se = 190 pm).[21] In addition, X-Ray crystal analysis of *N*-(o-bromophenyl)-thiazoline-2-selenone **6c** displays an angle of 131° between the endocyclic nitrogen atom and the methylene substituent borne in position 4 of the thiazoline ring, i.e. exactly the same value observed for *N*-(o-bromophenyl)-thiazoline-2-thione **1c** (Figure 2).

In this context, the computational study furnished obviously very close optimized GS and TS geometries for compounds of series **6** compared to those observed in series **1**, and the whole remarks already mentioned above may be transposed.

In contrast, the substitution of a thiocarbonyl group (series **1**) by a carbonyl group (series **7**) involved a significant impact on the value of barriers to rotation: a drastic decrease was observed, from 30 to 44 kJ/mol depending on the nature of the halogen.[22] As a consequence, isolation of both enantiomers of the fluoro derivative **7a** was not possible because of quick interconversion.[23] Indeed, the calculated rotational barrier was estimated at 56 kJ/mol, switching thus this compound into class I with respect to **1a** ranked into the intermediate class II. Contrary to all others series, the chloro and bromo structures **7b** and **7c**

[21] A. Bondi, *J. Phys. Chem.* **1964**, *68*, 441-451.

[22] Such structural modifications on atropisomers have already been reported in literature: a) E. M. Yilmaz, I. Dogan, *Tetrahedron*: *Asymmetry* **2008**, *19*, 2184-2191. b) Ö. Demir-Ordu, E. M. Yilmaz, I. Dogan, *Tetrahedron*: *Asymmetry* **2005**, *16*, 3752-3761. c) F. Oguz, I. Dogan, *Tetrahedron*: *Asymmetry* **2003**, *14*, 1857-1864.

[23] None enantiomers separation observed on the Whelk-O1 (*S,S*) column at 10 °C (Heptane/ethanol/dichloromethane - 70/20/10)

are part of class II, while the *N*-(o-iodophenyl)-thiazoline-2-one **7d** is located on the border class II/class III.

The DFT calculations revealed some notable aspects specific to the transition states of the oxo compounds **7**. Firstly, the values for the angle β are smaller of 4.7° on average by comparing the TS geometries of analogous structures from series **7** to series **1**; this can be attributed to the shorter C=O bond (120 pm for C=O vs 165 pm for C=S) generating less flexibility.[24] In addition, the TS geometries in series **7** are characterized by less distortion on the aromatic moiety with respect to the halogenated homologues in series **1** (e.g. C1'-C6'-C4'-C3' dihedral angle ψ for **7d**: 5.5° in TS1 and 6.1° in TS2, to be compared to 8.1° in TS1 and 8.0° in TS2 for **1d**), meaning a rotation process requiring less energy. Last but not least, contrary to all other series reported in this paper, the two transition states for the racemization of a given compound of the series **7** exhibit very close geometries on the thiazoline moiety as illustrating by the values of angle α (e.g. in TS1/TS2: 135.7°/134.5° for **7d**, to be compared to 135.9°/131.2° for **1d**), as well as for angle β (e.g. in TS1/TS2: 129.0°/127.9° for **7d**, to be compared to 134.5°/130.7° for **1d**). Consequently, although $\Delta G^{\neq}_{calc}$ militate in favour of pathway A in the cases of fluoro and chloro derivatives **7a** and **7b**, calculations do not discriminate the two rotation pathways A and B for **7c**, and support pathway B for **7d**.[25]

CONCLUSION

We reported the experimental and calculated rotational barriers of 22 *N*-Arylthiazolines exhibiting a large molecular diversity on the substituents located in the flanking positions of

[24] van der Waals radius for oxygen atom = 142 pm; see ref 21.

[25] Same trend observed with three different functional/basis sets (B3LYP/6-311G(3d,3p), M06-2X/6-311G(3d,3p) and PBE0/def2-TZVPP): see supporting information.

the chiral axis. Indeed, several types of structural modifications were considered on this same scaffold: substituting one group for another, swapping the position of flanking substituents around the chiral axis, or removing a group. The resulting rotational barriers (from ΔG_{rot} < 80 kJ/mol to ΔG_{rot} = 169 kJ/mol, i.e. $\Delta\Delta G_{rot}$ > 89 kJ/mol) allowed to accurately evaluate the impact of such modifications on enantiomeric stability. To go further in understanding the parameters involved, the two pathways of rotation around the pivotal bond were studied and discriminated by exploring the geometries of GS/TS with the help of X-Ray analysis and DFT calculations. This highlighted that the torsion on the aromatic ring in the transition state significantly impacted the value of the corresponding rotational barrier. The results described herein provide general trends on the structure-rotational barrier relationships which can be extrapolated to other atropisomeric series in order to modulate their enantiomeric stability thanks to judicious structural optimization. In particular, such data are very useful during design and optimization of catalysts or drugs with a chiral axis to end up with either a pair of fast exchanging rotamers or either a pair of atropisomers.

EXPERIMENTAL SECTION

General information

Unless specified, all reagents, starting materials and solvents were purchased from commercial sources and used as received. Melting points are uncorrected. Analytical thin-layer chromatography (TLC) was performed using precoated silica gel plates and visualization was achieved by UV light (254 nm). Flash chromatography was performed using silica gel and a gradient solvent system. ^{1}H and ^{13}C NMR spectra were measured on 400 MHz spectrometer with $CDCl_3$ as solvent. Chemical shifts (ppm) were recorded with respect to TMS in $CDCl_3$. Multiplicities are given as s (singlet), d (doublet), t (triplet), q (quartet), m (multiplet), dd (doublet of doublets) or ddd (doublet of doublets of doublets).

Coupling constants are reported as a *J* value in Hz. HRMS data were recorded on a mass spectrometer with electrospray ionization and TOF mass analyzer. Optical rotations were measured with a sodium lamp (589 nm) and a double-jacketed 10 cm cell at 25°C. The chiral HPLC analyses were performed on Agilent 1260 Infinity unit (pump G1311B, autosampler G1329B, DAD G1315D). The analytical column (250x4.6 mm) used is (*S*,*S*)-Whelk-O1 from Regis Technologies (Morton Grove, USA), except for **5a** (Daicel Chiralpak IE). Retention times Rt in minutes, retention factors $k_i = (Rt_i - Rt_0)/Rt_0$ and enantioselectivity factor $\alpha = k_2/k_1$ and resolution $Rs = 1.18 (Rt_2 - Rt_1) / (w_1 + w_2)$ are given. Preparative chiral separations were done with (*S*,*S*)-Whelk-O1 from Regis Technologies (Morton Grove, USA) with a mixture of Heptane/Ethanol/Chloroform (7/2/1) as mobile phase, except for **5a** (Daicel Chiralpak IE with Heptane/Ethanol, 9/1).

General synthesis of *N*-aryl-thiazoline-2-thione 2, 3, 4d and 5a

Distilled triethylamine (40 mmol) was added dropwise under nitrogen atmosphere to a solution of an *ortho*-substituted aniline (20 mmol) in carbon disulfide (38 mL). The mixture was stirred 24-48 h at r.t. Then the precipitate was filtered, washed with Et_2O and dried to give the dithiocarbamate salt. This salt was used without any further purification and immediately solubilised in acetonitrile (31 mL). 20 mmol of α-halogeno ketone/aldehyde (2-chlorocyclohexanone for series **2**, chloroacetone for series **3**, chloroacetaldehyde for **4d** and **5a**) were then added dropwise at r.t. under nitrogen atmosphere. The mixture was stirred 24 h at r.t. Then a 37% HCl solution (5 mL) was added dropwise and the mixture was heated at reflux (oil bath) for 20 minutes. The solvent was evaporated under reduced pressure and water was added (50 mL). The mixture was extracted with dichloromethane (3 x 50 mL), the organic layer was dried on $MgSO_4$ and evaporated under reduced pressure. The desired product was purified by flash chromatography (petroleum ether-dichloromethane, 100/0 → 0/100).

1a-d, **2a** and **3a** are known compounds and their ^{1}H NMR spectra are in accordance with literature data.[8,26]

3-(2-chlorophenyl)-3,4,5,6-tetrahydro-2*H*-cyclohexa[*d*][1,3]thiazole-2-thione 2b

Yield = 34%; Rf = 0.45 (petroleum ether/dichloromethane, 1/1); mp 127.1°C (racemate); ^{1}H NMR (400 MHz, $CDCl_3$) δ 1.76-1.84 (4H, m, 2 CH_2), 2.04-2.06 (2H, m, CH_2), 2.51-2.53 (2H, m, CH_2); 7.31-7.33 (1H, m, arom), 7.43-7.45 (2H, m, arom), 7.56-7.58 (1H, m, arom); ^{13}C NMR (100 MHz, $CDCl_3$) δ 21.6, 22.6, 24.3, 26.9, 120.8, 128.1, 130.2, 130.7, 130.9, 132.5, 135.1, 136.9, 188.0; HRMS (ESI/TOF) *m/z* $[M+H]^+$ Calcd for $C_{13}H_{13}NS_2Cl$: 282.0172; found: 282.0174; Chiral HPLC: Whelk-O1 (*S,S*), 25 °C, Heptane/ethanol 60/40, 1 mL/min, UV and CD 254 nm, Rt_1 = 6.71 min (+), Rt_2 = 8.15 min (-), k_1 = 1.24, k_2 = 1.72, α = 1.39 and Rs = 3.76; First eluted enantiomer (99.5% ee): $[\alpha]_D^{25}$ -16 (c 0.30, $CHCl_3$).

3-(2-bromophenyl)-3,4,5,6-tetrahydro-2*H*-cyclohexa[*d*][1,3]thiazole-2-thione 2c

Yield: 40%; Rf = 0.36 (petroleum ether/dichloromethane, 1/1); mp 132.0°C (racemate); ^{1}H NMR (400 MHz, $CDCl_3$) δ 1.79-1.86 (4H, m, 2 CH_2), 2.00-2.06 (2H, m, CH_2), 2.52-2.54 (2H, m, CH_2), 7.32-7.41 (2H, m, arom), 7.49-7.51 (1H, m, arom), 7.73-7.75 (1H, m, arom); ^{13}C NMR (100 MHz, $CDCl_3$) δ 21.1, 22.1, 22.7, 24.0, 120.2, 121.8, 128.4, 129.8, 130.6, 133.2, 136.2, 136.4, 186.9; HRMS (ESI/TOF) *m/z* $[M+H]^+$ Calcd for $C_{13}H_{13}NS_2Br$: 325.9667; found: 325.9666; Chiral HPLC: Whelk-O1 (*S,S*), 25 °C, Heptane/ethanol 60/40, 1 mL/min, UV and polarimeter, Rt_1 = 7.00 min (-), Rt_2 = 8.43 min (+), k_1 = 1.33, k_2 = 1.81, α = 1.36 and Rs = 3.60; First eluted (99% ee): $[\alpha]_D^{25}$ 21 (c 0.79, $CHCl_3$).

[26] A. Iida, M. Matsuoka, H. Hasegawa, N. Vanthuyne, D. Farran, C. Roussel, O. Kitagawa, *J. Org. Chem.* **2019**, *84*, 3169-3175.

3-(2-iodophenyl)-3,4,5,6-tetrahydro-2*H*-cyclohexa[*d*][1,3]thiazole-2-thione 2d

Yield: 48%; Rf = 0.43 (petroleum ether/dichloromethane, 1/1); mp 157.0°C (racemate); ^{1}H NMR (400 MHz, $CDCl_3$) δ 1.75-1.90 (4H, m, 2 CH_2), 2.00-2.11 (2H, m, CH_2), 2.51-2.60 (2H, m, CH_2), 7.20 (1H, dd, *J* = 1.6, 7.8, arom), 7.30 (1H, dd, *J* = 1.5, 7.8, arom), 7.52 (1H, dd, *J* = 1.2, 7.6, arom), 7.98 (1H, dd, *J* = 1.5, 8.0, arom); ^{13}C NMR (100 MHz, $CDCl_3$) δ 21.7, 22.7, 23.3, 25.0, 98.0, 121.1, 129.6, 129.7, 130.9, 136.5, 140.2, 140.5, 187.6; HRMS (ESI/TOF) *m/z* $[M+H]^+$ Calcd for $C_{13}H_{13}NS_2I$: 373.9529; found: 373.9532; Chiral HPLC: Whelk-O1 (*S,S*), 25 °C, Heptane/ethanol 60/40, 1 mL/min, UV and polarimeter, Rt_1 = 7.35 min (-), Rt_2 = 8.94 min (+), k_1 = 1.45, k_2 = 1.98, α = 1.36 and Rs = 3.82; First eluted (99.5% ee): $[\alpha]_D^{25}$ 86 (c 0.73, $CHCl_3$).

3-(2-chlorophenyl)-4-methylthiazole-2(3*H*)-thione 3b

Yield: 80%; Rf = 0.76 (dichloromethane/AcOEt, 9/1); mp 150-152°C (racemate); ^{1}H NMR (400 MHz, $CDCl_3$) δ 1.94 (3H, s, CH_3), 6.36 (1H, s, CH), 7.31 (1H, m, arom), 7.45-7.52 (2H, m, arom), 7.59-7.64 (1H, m, arom); ^{13}C NMR (100 MHz, $CDCl_3$) δ 15.6, 106.5, 128.5, 130.5, 131.0, 131.3, 132.8, 135.6, 139.6, 190.2; HRMS (ESI/TOF) *m/z* $[M+H]^+$ Calcd for $C_{10}H_9NS_2Cl$: 241.9859; found: 241.9855; Chiral HPLC: Whelk-O1 (*S,S*), 25 °C, Heptane/ethanol/dichloromethane 50/30/20, 1 mL/min, UV and CD 254 nm, Rt_1 = 4.43 min (+), Rt_2 = 4.97 min (-), k_1 = 0.50, k_2 = 0.68, α = 1.36 and Rs = 2.62; First eluted (99% ee): $[\alpha]_D^{25}$ 25 (c 0.51, $CHCl_3$).

3-(2-bromophenyl)-4-methylthiazole-2(3*H*)-thione 3c

Yield: 46%; Rf = 0.76 (dichloromethane/AcOEt, 9/1); mp 163-165°C (racemate); ^{1}H NMR (400 MHz, $CDCl_3$) δ 1.94 (3H, d, *J* = 1.1, CH_3), 6.36 (1H, q, *J* = 1.1, CH), 7.33 (1H, dd, *J* = 1.5, 7.8, arom), 7.41 (1H, ddd, *J* = 1.6, 7.6, 7.9, arom), 7.53 (1H, ddd, *J* = 1.3, 7.6, 7.7, arom), 7.79 (1H, dd, *J* = 1.2, 8.0, arom);

^{13}C NMR (100 MHz, $CDCl_3$) δ 15.8, 106.5, 122.9, 129.9, 130.5, 131.5, 134.3, 137.3, 139.5, 190.1; HRMS (ESI/TOF) *m/z* $[M+H]^+$ Calcd for $C_{10}H_9NS_2Br$: 287.9333; found: 287.9333; Chiral HPLC: Whelk-O1 (*S,S*), 25 °C, Heptane/ethanol/dichloromethane 50/30/20, 1 mL/min, UV and CD 254 nm, Rt_1 = 4.53 min (+), Rt_2 = 5.07 min (-), k_1 = 0.54, k_2 = 0.72, α = 1.34 and Rs = 2.66; First eluted (99% ee): $[\alpha]_D^{25}$ 85 (c 0.44, $CHCl_3$).

3-(2-iodophenyl)-4-methylthiazole-2(3*H*)-thione 3d

Yield: 49%; Rf = 0.76 (dichloromethane/AcOEt, 9/1); mp 193-195°C (racemate); ^{1}H NMR (400 MHz, $CDCl_3$) δ 1.93 (3H, d, *J* = 1.1, CH_3), 6.37 (1H, q, *J* = 1.1, CH), 7.23 (1H, ddd, *J* = 1.5, 7.6, 7.9, arom), 7.30 (1H, dd, *J* = 1.4, 7.8, arom), 7.56 (1H, ddd, *J* = 1.3, 7.6, 7.8, arom), 8.01 (1H, dd, *J* = 1.2, 8.0, arom); ^{13}C NMR (100 MHz, $CDCl_3$) δ 16.1, 98.3, 106.7, 129.8, 130.0, 131.3, 139.3, 140.5, 140.8, 189.7; HRMS (ESI/TOF) *m/z* $[M+H]^+$ Calcd for $C_{10}H_9NS_2I$: 333.9216; found: 333.9220; Chiral HPLC: Whelk-O1 (*S,S*), 25 °C, Heptane/ethanol/dichloromethane 50/30/20, 1 mL/min, UV and CD 254 nm, Rt_1 = 4.69 min (-), Rt_2 = 5.24 min (+), k_1 = 0.59, k_2 = 0.77, α = 1.32 and Rs = 2.68; First eluted (99% ee): $[\alpha]_D^{25}$ 174 (c 0.47, $CHCl_3$).

3-(2-iodophenyl)thiazole-2(3*H*)-thione 4d

Yield: 32%; Rf = 0.61 (dichloromethane); ^{1}H NMR (400 MHz, $CDCl_3$) δ 6.71 (1H, d, *J* = 4.6, arom), 6.98 (1H, d, *J* = 4.6, arom), 7.21 (1H, ddd, *J* = 1.5, 7.7, 7.9, arom), 7.40 (1H, dd, *J* = 1.4, 7.9, arom), 7.52 (1H, ddd, *J* = 1.4, 7.9, arom), 7.99 (1H, d, *J* = 1.1, 7.9, arom); ^{13}C NMR (100 MHz, $CDCl_3$) δ 96.7, 111.7, 129.3, 129.8, 131.4, 131.5, 140.4, 141.5, 189.0; HRMS (ESI/TOF) *m/z* $[M+H]^+$ Calcd for $C_9H_7NS_2I$: 319.9059; found: 319.9057.

3-(2-fluoro-6-methylphenyl)thiazole-2(3*H*)-thione 5a

Yield: 61%; Rf = 0.64 (dichloromethane); mp 117.0°C (racemate); ^{1}H NMR (400 MHz, $CDCl_3$) δ 2.23 (3H, s, CH_3), 6.72 (1H, d, *J* = 4.7, arom), 6.95 (1H, d, *J* = 4.5, arom), 7.10 (1H, dd, *J* = 8.4, 9.3, arom), 7.15 (1H, d, *J* = 7.7, arom), 7.38 (1H, ddd, *J* = 5.6, 7.7, 8.2, arom); ^{13}C NMR (100 MHz, $CDCl_3$) δ 17.7 (d, *J* = 2.3), 111.9, 114.3 (d, *J* = 19.4), 125.7 (d, *J* = 13.3), 126.5 (d, *J* = 3.5), 131.1 (d, *J* = 8.3), 131.4, 138.6, 157.7 (d, *J* = 253.4), 189.2; HRMS (ESI/TOF) *m/z* $[M+H]^+$ Calcd for $C_{10}H_9NFS_2$: 226.0155; found: 226.0152; Chiral HPLC: Chiralpak IE, 25 °C, Heptane/ethanol 90/10, 1 mL/min, UV and CD 254 nm, Rt_1 = 10.30 min (-), Rt_2 = 11.73 min (+), k_1 = 2.43, k_2 = 2.91, α = 1.20 and Rs = 3.77; First eluted (99.5% ee): $[\alpha]_D^{25}$ -148 (c 1.11, $CHCl_3$).

General synthesis of *N*-aryl-thiazoline-2-selenone 6

Iodomethane (7 mmol) was added under nitrogen atmosphere to a solution of *N*-aryl-thiazoline-2-thione (1.40 mmol) in acetone (6.5 mL). The mixture was stirred 2-3 h at r.t. Then the precipitate was filtered, washed with acetone and dried to give the thiazolium salt. This salt (0.37 mmol) was used without any further purification and immediately solubilised in acetonitrile (3 mL). This mixture was added dropwise to a solution of selenium powder (0.73 mmol) and sodium borohydride (0.81 mmol) in anhydrous ethanol (13 mL). After stirring for 30 min, a solution of acetic acid in water (5 mol %) was added dropwise, the precipitate was filtered off and washed with dichloromethane. The aqueous layer was separate from the filtrate and extracted with dichloromethane (3 x 50 mL). The combined organic layers were washed with water (3 x 50 mL), dried on $MgSO_4$ and evaporated under reduced pressure. The desired product was purified by flash chromatography (petroleum ether-dichloromethane, 100/0 → 0/100).

3-(2-fluorophenyl)-3,4,5,6-tetrahydro-2*H*-cyclopenta[*d*][1,3]thiazole-2-selenone 6a

Yield: 32% ; brown solid; mp 163.0-165.0°C (racemate); ^{1}H NMR (400 MHz, $CDCl_3$) δ 2.49-2.62 (4H, m, 2 CH_2), 2.75-2.81 (2H, m, CH_2), 7.27-7.34 (2H, m, arom), 7.44-7.54 (2H, m, arom); ^{13}C NMR (100 MHz, $CDCl_3$) δ 26.1, 27.1, 28.1, 117.2 (d, *J* = 19.0), 124.9 (d, *J* = 3.7), 126.3 (d, *J* = 12.4), 128.2, 129.7, 131.6 (d, *J* = 7.5), 148.8, 156.6 (d, *J* = 253.0), 187.8; ^{19}F NMR (376,5 MHz, $CDCl_3$) δ -120.0; HRMS (ESI/TOF) *m/z* $[M+H]^+$ Calcd for $C_{12}H_{11}NFSSe$: 299.9756; found: 299.9756.

3-(2-chlorophenyl)-3,4,5,6-tetrahydro-2*H*-cyclopenta[*d*][1,3]thiazole-2-selenone 6b

Yield: 9%; brown oil; ^{1}H NMR (400 MHz, $CDCl_3$) δ 2.45-2.58 (4H, m, 2 CH_2), 2.77-2.82 (2H, m, CH_2), 7.43-7.62 (4H, m, arom); ^{13}C NMR (100 MHz, $CDCl_3$) δ 26.4, 27.3, 28.3, 128.3, 128.8, 129.8, 131.0, 131.3, 131.7, 136.4, 148.8, 186.7; HRMS (ESI/TOF) *m/z* $[M+H]^+$ Calcd for $C_{12}H_{11}NSClSe$: 315.9458; found: 315.9462; Chiral HPLC: Whelk-O1 (*S,S*), 10°C, Heptane/ethanol 60/40, 1 mL/min, UV and polarimeter, Rt_1 = 6.96 min (+), Rt_2 = 8.07 min (-), k_1 = 1.32, k_2 = 1.69, α = 1.28 and Rs = 3.44; First eluted (99.5% ee): $[\alpha]_D^{25}$ -91 (c 0.15, $CHCl_3$).

3-(2-bromophenyl)-3,4,5,6-tetrahydro-2*H*-cyclopenta[*d*][1,3]thiazole-2-selenone 6c

Yield: 32%; yellow solid; mp 174.5-176.2°C (racemate); ^{1}H NMR (400 MHz, $CDCl_3$) δ 2.40-2.60 (4H, m, 2 CH_2), 2.75-2.82 (2H, m, CH_2), 7.36-7.43 (2H, m, arom), 7.46-7.54 (1H, m, arom), 7.74-7.77 (1H, m, arom); ^{13}C NMR (100 MHz, $CDCl_3$) δ 26.2, 27.3, 28.2, 121.4, 128.2, 128.9, 129.8, 131.3, 134.0, 138.1, 148.4, 187.1; HRMS (ESI/TOF) *m/z* $[M+H]^+$ Calcd for $C_{12}H_{11}NSBrSe$: 359.8952; found: 359.8948; Chiral HPLC: Whelk-O1 (*S,S*), 25 °C, Heptane/ethanol 60/40, 1 mL/min, UV and CD 254 nm, Rt_1 = 7.93 min (-), Rt_2 = 9.14 min (+), k_1 = 1.69, k_2 = 2.10, α = 1.24 and Rs = 3.10; First eluted (99.5% ee): $[\alpha]_D^{25}$ -22 (c 0.18, $CHCl_3$).

3-(2-iodophenyl)-3,4,5,6-tetrahydro-2*H*-cyclopenta[*d*][1,3]thiazole-2-selenone 6d

Yield: 11%; yellow solid; mp 184.5-186.8°C (racemate); ^{1}H NMR (400 MHz, $CDCl_3$) δ 2.39-2.58 (4H, m, 2 CH_2), 2.73-2.85 (2H, m, CH_2), 7.23 (1H, dd, *J* = 1.6, 7.8, arom), 7.36 (1H, dd, *J* = 1.6, 8.0, arom), 7.53 (1H, dd, *J* = 1.3, 7.7, arom), 8.0 (1H, dd, *J* = 1.6, 8.0, arom); ^{13}C NMR (100 MHz, $CDCl_3$) δ 26.5, 27.8, 28.4, 96.8, 128.7, 129.2, 130.0, 131.4, 140.5, 141.8, 148.3, 187.0; HRMS (ESI/TOF) *m/z* $[M+H]^+$ Calcd for $C_{12}H_{11}NSISe$: 407.8816; found: 407.8814; Chiral HPLC: Whelk-O1 (*S,S*), 25 °C, Heptane/ethanol 60/40, 1 mL/min, UV and CD 254 nm, Rt_1 = 8.25 min (-), Rt_2 = 9.53 min (+), k_1 = 1.80, k_2 = 2.23, α = 1.24 and Rs = 3.58; First eluted (99.5% ee): $[\alpha]_D^{25}$ 26 (c 0.07, $CHCl_3$).

General synthesis of *N*-aryl-thiazoline-2-one 7

Iodomethane (7.50 mmol) was added under nitrogen atmosphere to a solution of an *N*-aryl-thiazoline-2-thione (1.50 mmol) in acetone (5 mL). The mixture was stirred 2-3 h at r.t. Then the precipitate was filtered, washed with acetone and dried to give the thiazolium salt. This salt (0.61 mmol) was used without any further purification and immediately solubilised in methanol (6.60 mL). A solution of sodium methoxide (0.61 mmol) in methanol (24 mL) was then added at r.t. under nitrogen atmosphere. The mixture was stirred 12 h at r.t. Water was added (100 mL) and the mixture was extracted with ethyl acetate (3 x 100 mL), the organic layer was dried on $MgSO_4$ and evaporated under reduced pressure. The desired product was purified by flash chromatography (dichloromethane-ethyl acetate, 100/0 → 60/40).

3-(2-fluorophenyl)-3,4,5,6-tetrahydro-2*H*-cyclopenta[*d*][1,3]thiazol-2-one 7a

Yield: 34%; colorless oil; ^{1}H NMR (400 MHz, $CDCl_3$) δ 2.22-2.32 (2H, m, CH_2), 2.47-2.57 (2H, m, CH_2), 2.75-2.84 (2H, m, CH_2), 7.19-7.27 (2H, m, arom), 7.32-7.42 (2H, m, arom); ^{13}C NMR (100 MHz, $CDCl_3$)

δ 23.4, 27.8 (d, *J* = 2.0 Hz), 29.3, 112.3, 117.0 (d, *J* = 19.8), 124.0 (d, *J* = 13.1), 124.9 (d, *J* = 4.3), 129.4, 130.5 (d, *J* = 7.7), 136.6, 157.6 (d, *J* = 251.0), 175.0; ^{19}F NMR (376,5 MHz, $CDCl_3$) δ -120.1; HRMS (ESI/TOF) *m/z* $[M+H]^+$ Calcd for $C_{12}H_{11}NOSF$: 236.0540; found: 236.0541; Chiral HPLC: Whelk-O1 (*S,S*), 10 °C, Heptane/ethanol/dichloromethane 70/20/10, 1 mL/min, UV and polarimeter, Rt = 7.81 min.

3-(2-chlorophenyl)-3,4,5,6-tetrahydro-2*H*-cyclopenta[*d*][1,3]thiazol-2-one 7b

Yield: 43%; colorless oil; ^{1}H NMR (400 MHz, $CDCl_3$) δ 2.15-2.24 (2H, m, CH_2), 2.30-2.46 (2H, m, CH_2), 2.65-2.79 (2H, m, CH_2), 7.24-7.37 (3H, m, arom), 7.43-7.49 (1H, m, arom); ^{13}C NMR (100 MHz, $CDCl_3$) δ 23.3, 27.7, 29.2, 112.0, 127.8, 129.8, 130.3, 130.6, 132.6, 133.9, 136.3, 174.8; HRMS (ESI/TOF) *m/z* $[M+H]^+$ Calcd for $C_{12}H_{11}NOSCl$: 252.0244; found: 252.0247; Chiral HPLC: Whelk-O1 (*S,S*), 25 °C, Heptane/ethanol 60/40, 1 mL/min, UV and polarimeter, Rt_1 = 5.93 min , Rt_2 = 8.69 min, k_1 = 0.98, k_2 = 1.90, α = 1.94 and Rs = 7.65; First eluted (99.5% ee): $[\alpha]_D^{25}$ 7 (c 0.28, $CHCl_3$).

3-(2-bromophenyl)-3,4,5,6-tetrahydro-2*H*-cyclopenta[*d*][1,3]thiazol-2-one 7c

Yield: 36%; brown oil; ^{1}H NMR (400 MHz, $CDCl_3$) δ 2.19-2.32 (2H, m, CH_2), 2.34-2.54 (2H, m, CH_2), 2.77-2.83 (2H, m, CH_2), 7.29-7.34 (2H, m, arom), 7.40-7.44 (1H, m, arom), 7.71 (1H, dd, *J* = 1.2, 8.0, arom); ^{13}C NMR (100 MHz, $CDCl_3$) δ 23.3, 27.7, 29.2, 112.0, 122.8, 128.6, 130.0, 130.7, 133.8, 135.7, 136.2, 174.8; HRMS (ESI/TOF) *m/z* $[M+Na]^+$ Calcd for $C_{12}H_{10}NOSBrNa$: 319.9538; found: 319.9539; Chiral HPLC: Whelk-O1 (*S,S*), 25 °C, Heptane/ethanol 60/40, 1 mL/min, UV and polarimeter, Rt_1 = 6.52 min (+), Rt_2 = 9.80 min (-), k_1 = 1.17, k_2 = 2.27, α = 1.94 and Rs = 8.07; First eluted (99.5% ee): $[\alpha]_D^{25}$ 16 (c 0.96, $CHCl_3$).

3-(2-iodophenyl)-3,4,5,6-tetrahydro-2*H*-cyclopenta[*d*][1,3]thiazol-2-one 7d

Yield: 67% ; yellow solid; mp 148.5-150.2°C (racemate); ^{1}H NMR (400 MHz, $CDCl_3$) δ 2.20-2.30 (2H, m, CH_2), 2.30-2.41 (1H, m, CH_2), 2.41-2.52 (1H, m, CH_2), 2.72-2.87 (2H, m, CH_2), 7.14 (1H, ddd, *J* = 1.6, 7.6, 8.0, arom), 7.29 (1H, dd, *J* = 1.5, 7.8, arom), 7.45 (1H, ddd, *J* = 1.3, 7.5, 7.9, arom), 7.93 (1H, dd, *J* = 1.2, 8.0, arom); ^{13}C NMR (100 MHz, $CDCl_3$) δ 23.3, 27.8, 29.6, 98.1, 112.1, 129.3, 129.4, 130.7, 135.8, 139.2, 139.9, 174.6; HRMS (ESI/TOF) *m/z* $[M+H]^+$ Calcd for $C_{12}H_{11}NOSI$: 343.9601; found: 343.9600; Chiral HPLC: Whelk-O1 (*S,S*), 25 °C, Heptane/ethanol 60/40, 1 mL/min, UV and polarimeter, Rt_1 = 6.87 min (+), Rt_2 = 9.98 min (-), k_1 = 1.29, k_2 = 2.33, α = 1.81 and Rs = 7.00; First eluted (99.5% ee): $[\alpha]_D^{25}$ 35 (c 0.93, $CHCl_3$).

Supporting Information Available

Copies of ^{1}H NMR, ^{13}C NMR and ^{19}F NMR spectra for all new compounds. Kinetic experiments and determination of rotational barriers (with solvent and temperature). Calculated rotational barriers obtained with B3LYP/6-311G(3d,3p), M06-2X/6-311G(3d,3p) and PBE0/def2-TZVPP methods. X-Ray data for compound (S_a)-**1c**, (S_a)-**2c** (S_a)-**3c** (S_a)-**6c**. ECD and UV spectra for compounds exhibiting a $\Delta G^{\neq}_{rot}$ > 100kJ/mol. Selected geometrical parameters (angle, dihedral angle, bond length) obtained from PBE0/def2-TZVPP method for GS and both TS of all compounds.

Acknowledgments

We thank Dr. M. Giorgi (Spectropole) for X-ray structures, and the « Centre Régional de Compétences en Modélisation Moléculaire de Marseille » for computing facilities.